Isolation, X-ray structure and properties of an unusual pentacarbonyl(2,2′-pyridyl-quinoxaline) tungsten complex

Irene Veroni [a], Christiana A. Mitsopoulou [a,*], Fernando J. Lahoz [b]

[a] *Inorganic Chemistry Laboratory, Department of Chemistry, National and Kapodistrian University of Athens, Panepistimiopolis, Zografou 15771, Greece*
[b] *Departamento de Quimica Inorganicas ICMA, Facultad de Ciencias, Universidad de Zaragozas CSIC, Zaragoza 50009, Spain*

Abstract

The first example of a monodentate complexation of 2-(2′-pyridyl)quinoxaline (**pq**) to a metal centre through N_4 is reported. Photochemical exchange of the THF ligand in $W(CO)_5THF$ by pq yields $W(CO)_5(N_4\text{-pq})$ (**1**), where the potentially bidentate **pq** ligand coordinates in an unusual monodentate fashion. Complex **1** is isolated as orange crystals and fully characterized on the basis of NMR, IR, UV–Vis and emission spectroscopy. The structure of **1** was determined by X-ray analysis. $W(CO)_5(N_4\text{-pq})$ (**1**) crystallizes in space group $P2_{1/n}$, monoclinic crystal system with $\alpha = 7.0237(5)$ Å, $b = 10.4618(8)$ Å, $c = 23.7768(18)$ Å, $Z = 4$ and $V = 1731.9(2)$ Å^3. Complex **1** exhibits intramolecular CH$\cdots$N and intermolecular CH$\cdots$O hydrogen bonds between the CH groups and nitrogen atoms of quinoxaline and CH groups and oxygen atoms of carbonyls, respectively, resulting in a supramolecular architecture in solid state. The preference to N_4 as coordination site is discussed in terms of electronic interactions. Solutions of **1** emits dually at 77 K while they are moderately instable at room temperature, as **1** undergoes chelation via a first-order kinetic process to form $W(CO)_4pq$ (**2**). The determined reaction rate of **1** in toluene is 2.3×10^{-5} s^{-1} (at 298 K) and is compared with literature values for other $W(CO)_5L$ (L:diimine) complexes.
© 2006 Elsevier B.V. All rights reserved.

Keywords: 2-(2′-Pyridyl)quinoxaline; Pentacarbonyl; Tungsten; Crystal structure; Hydrogen bonds; Emission

1. Introduction

The quinoxaline class of ligands can meet modern expectations of metallo-organic chemistry, as they own low-lying LUMOs, contain two nitrogen atoms in the suitable for bridges *para*-position and can be easily functionalized, allowing us to tailor their properties [1]. Besides, quinoxaline structure is recognized in a great number of naturally occurring compounds such as riboflavin (vitamin B$_2$), flavoenzymes, molybdopterines and antibiotics of streptomyces type that are implicated in considerable intra- and inter-electron transfer biochemical processes. Quinoxaline derivatives can be used, from the one hand, as antibacterial, antiviral, anticancer, antifungal, antihelmintic and insecticidalagents [2] and from the other, as electron-withdrawing groups in p-conjugated polymer chemistry [3], as fluorescent dyes [4] or as optical-based sensors for anions in organic media [5].

2-(2′-Pyridyl)quinoxaline (**pq**) (Scheme 1) is a synthetic product – produced by an unexpected condensation reaction [6] – that is a variation on the commonly used bridging ligand 2,3-bis (2-pyridyl)quinoxaline (dpq). Pq combines the bridging properties of quinoxalines along with the chelating efficiency of 2-2-bpy. Up until now, a plethora of metal complexes have been reported, where pq is bi-coordinated through N_1 and N_1' atoms [7], but there has never been any undoubted proof for coordination of the metal at N_4. In spite of that, semi-empirical calculations have shown that the HOMO of pq is mostly a 'lone' electron pair on N_1 and N_4 [7n], thus these two nitrogen atoms should share almost the same propensity for coordination. The thermodynamic stability that offers the chelation of pq after its coordination at N_1 should be the major reason for the above experimental observation.

* Corresponding author. Tel.: +30 210 7274 452; fax: +30 210 8322828.
E-mail address: cmitsop@chem.uoa.gr (C.A. Mitsopoulou).
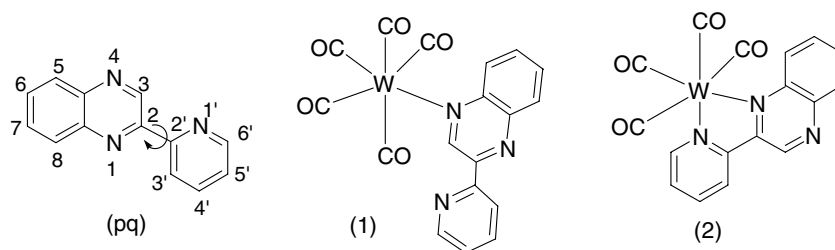
Scheme 1.

On the other hand, organometallic complexes between transition metal carbonyls and N-containing heterocycles have been the subject of considerable interest in recent years. Their photochemical and electronic properties and potential for industrial applications have led to many studies for use as photosensitizers, catalysts and conducting coordinating polymers [8]. Moreover, the importance of asymmetrical transition metal complexes, namely $M(CO)_5L$ where M = Cr, W and L = π-conjugated ligand, in the field of second-order NLO materials is now very well documented [9]. Up until now in the literature several pentacarbonyl d^6 metal diimine complexes have been observed either as mere intermediates in photolysis processes of group 6 metal hexacarbonyls in the presence of the potentially bidentate diimine type ligands [10], or as isolated products after substitution reactions of various photo-generated $M(CO)_5(\sigma$-donor) complexes [11]. Apart from a few cases [12], most of these complexes are thermally unstable in solution yielding the corresponding tetracarbonyl complexes.

Herein, we offer the first example of a metal complex where pq is mono-coordinated through N_4, by reporting the synthesis and characterization of the complex $W(CO)_5(N_4$-pq) (**1**) (Scheme 1). The ^{15}N spectrum of free pq aims at the understanding of the distribution of atomic partial charges, before the ligand's complexation. The crystal structure of **1** is quite unique in the sense that as far as we know there are no published crystal structures of metal complexes of the type $M(CO)_5$(diimine) – with M standing for Cr, Mo or W – where the usually chelated diimine is mono-coordinated. It is also the first time that pq is unambiguously proved to be coordinated by N_4 atom. Growing crystals of **1** was quite a challenge, as this is the intermediate en route to $W(CO)_4$pq (**2**) [13] (Scheme 1) in solution. The kinetics of the transformation of **1–2** in toluene have been investigated by UV–Vis spectroscopy and the corresponding k_{obsd} has been induced.

The numbering of atoms for both complexes **1** and **2** is kept in accordance with **pq** throughout the text (Scheme 1) except of the section of crystal data.

2. Experimental

2.1. Materials and equipment

2,2′-pq was synthesized following Hadjiliadis routine [6]. The complex $W(CO)_6$ along with THF, which was used in synthesis, were obtained from Aldrich Chemicals and used after being dried. The solvents used in UV–Vis studies were purified to spectroscopic quality by standard methods [14]. The deuterated solvents, which were utilized in NMR experiments, were purchased from Aldrich and were of 99.99% purity.

Photolysis experiment was carried out with the 1000 W xenon lamp in an Oriel, mod 68820, Universal Arc. Lamp source selected with appropriate interference filter (Corning). FT-IR spectra in solution and in KBr pellets were recorded on a Nicolet Magna IR 560 spectrophotometer having $1.0 \, cm^{-1}$ resolution. Electronic absorption spectra were recorded on a Varian Cary 300 spectrometer, having a circulating thermostat. The solute concentration was $\approx 10^{-5}$ M and the samples were prepared just before the measurements. ^{1}H NMR measurements were performed using a Varian Unity Plus 300 NMR spectrometer. Samples were run in a 5 mm probe with deuterated solvents as internal lock and reference. The $^{15}N–^{1}H$ HMBC spectra were recorded in a Varian INOVA-500 MHz NMR spectrometer using NH_3 as external standard. Microanalyses were performed with a Euro Vector EA 3000 analyzer. Emission measurements of **1** were performed in a 2-MeTHF glass at 80 K, using an Edinburgh Instruments FS-900 apparatus. Emission spectra were registered with a Xe lamp as the excitation source. Lifetime measurements were performed in single photon counting mode, with a nanosecond flash lamp as the excitation source.

2.2. Synthesis of $W(CO)_5(N_4$-pq) (**1**)

A tetrahydrofuran solution (50 mL) of the parent tungsten hexacarbonyl (1 mmol) was deoxygenated by continuous nitrogen purging and then irradiated with a 1000 W xenon lamp at 25 °C for 20 min. An approximately 10% excess amount of pq was then added to the reaction vessel and the irradiation was continued for 10 more minutes. The tetrahydrofuran was slowly evaporated under atmospheric pressure and the residue was passed through a silica gel column using hexane as the eluent. After the slow evaporation of hexane, complex **1** was received as an orange solid in 70% yield. Anal. Calcd. for $C_{18}H_9N_3O_5W$: C, 40.60; H, 1.72; N, 7.91; O, 15.12; W, 34.81. Found: C, 40.70; H, 1.71; N, 7.89; O, 15.00%. IR (in DCM): $\tilde{\nu}_{co}/cm^{-1}$ 2073 (w), 1932 (st) and 1904 (m). NMR data for **1** are included in Table 1.

Table 1
^{1}H NMR chem. shifts of **1**, **2** and **pq** in CDCl$_3$

	H$_3$	H$_{6'}$	H$_{3'}$	H$_5$	H$_8$	H$_{4'}$	H$_6$	H$_7$	H$_{5'}$
pq	9.98	8.80	8.62	8.19	8.18	7.92	7.82	7.79	7.43
1	10.61	8.83	8.66	8.61	8.24	7.97	7.94	7.92	7.47
2	9.59	9.56	8.52	8.26	9.32	8.13	8.04	8.00	7.55

2.3. X-ray crystallography of **1**

Orange needles of **1** suitable for X-ray structural determination were grown by slow evaporation from a mixture of *n*-hexane–dichloromethane (4:1) at 279 K. Details of the crystal data, data collection, and structure refinement parameters for **1** are given in Table 2. Single-crystal X-ray diffraction experiments were carried out on a Bruker SMART APEX CCD diffractometer with graphite monochromated Mo Kα radiation at 100 K. The semi-empirical method SADABS [15] was applied for absorption correction. The structure was solved by direct methods and refined by the full-matrix least-squares technique against F^2 with anisotropic temperature parameters for all non-hydrogen atoms. Data reduction and further calculations were performed using the SAINT [16] and SHELXTL-97 [17] program packages.

3. Results and discussion

W(CO)$_5$pq **1** can be prepared either via the tetrahydrofuran complex, W(CO)$_5$(THF) (Reactions 1 and 2, Scheme 2) or directly (Reaction 3, Scheme 2).

The first synthetic route is based on the method of Strohmeier and Müller [18] and includes the photolysis of tungsten hexarbonyl in THF, yielding the mononuclear THF adduct W(CO)$_5$(THF). Further photochemical reac-

Table 2
Crystallographic data for **1**

Compound	**1**
Formula	C$_{18}$H$_9$N$_3$O$_5$W
Molecular weight	531.13
Crystal system	Monoclinic
Space group	P2$_1$/c
a (Å)	7.0237(5)
b (Å)	10.4618(8)
c (Å)	23.7768(18)
α (°)	90.00
β (°)	97.5650(10)
γ (°)	90.00
V (Å^3)	1731.9(2)
Z	4
T (K)	100(2)
θ$_{max}$ (°)	26.16
μ (Mo Kα λ = 0.71073 Å)	6.706 (mm^{-1})
Number of unique reflections (R$_{int}$)	4985 (0.0518)
Number of observed reflections (I > 2σ(I))	3223
Number of parameters	280
R$_1$ (on F for observed reflections)	0.0315
wR$_2$ (on F2 for all reflections)	0.0660

tion of the latter with an excess of pq after a short irradiation time (about 10 min), gives an orange solution that contains **1**. Alternatively, the synthesis of the THF adduct is bypassed and direct photolysis of 5 mmol of the quinoxaline derivative with 1 mmol of tungsten hexacarbonyl in dry hexane is used, but only a moderate yield is achieved – thus this method was abandoned in favor of the first.

Whether the formation of **1** is a merely photochemical process or not was examined by recording the absorption spectra of W(CO)$_5$(THF) in THF solvent after the addition of pq. In Fig. 1, we observe the gradual decay of the bands at 419 and 455 nm that are related to W(CO)$_5$(THF) and the concomitant small growth of the band at 586 nm that corresponds to the MLCT band of complex **2** [13].

There is not a clear indication of the formation of **1**, except perhaps from the fact that the isosbestic point at 507 nm is not particularly sharp. As a consequence, we conclude that either the thermal path of the reaction of W(CO)$_5$(THF) with pq is different from the photochemical one or although **1** is formed thermally, it decomposes very quickly.
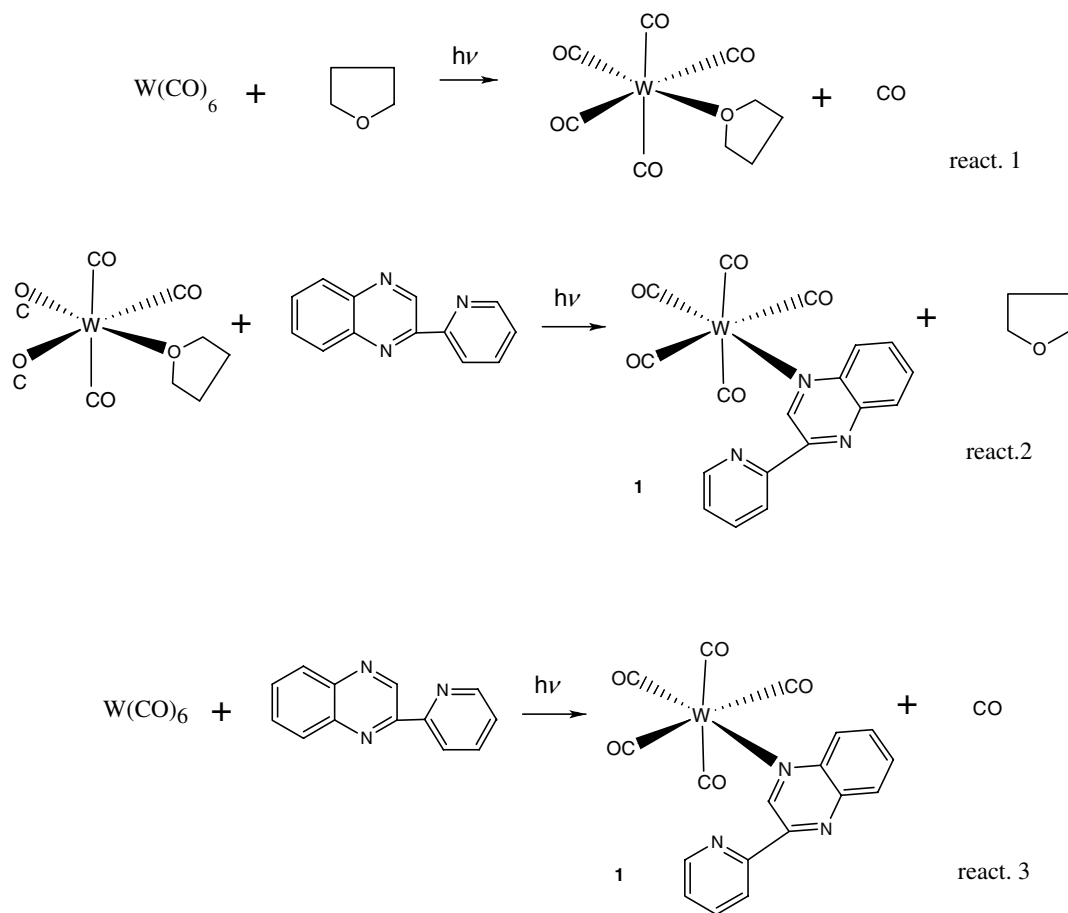
A first indication of the coordination site of pq to W(CO)$_5$ fragment is provided both by the ^{1}H NMR and the HMBC ^{1}H–^{15}N spectra of **1**. A comparison of ^{1}H NMR chemical shifts of **1**, **2** [13] and **pq** (Table 1) indicates that ^{1}H chemical shifts in pyridyl moiety of pq are almost unaffected from the coordination to W(CO)$_5$ (**1** vs **pq**).

On the contrary, as far as the quinoxaline moiety in **1** is concerned, a downfield shift of its protons is observed due to the paratropic effect of the tungsten moiety. Actually, the proton atom which is most deshielded, is the H$_3$ (0.63 ppm compared to the one of the free pq) indicating that this is the closest one to the metal centre. Moreover, after complexation the peaks of H$_5$ and H$_8$ are well-separated; H$_5$ is considerably more deshielded than H$_8$ after pq's coordination to the W(CO)$_5$ fragment. In contrast, in bidentate complex **2** [13] considerable changes in the chemical shifts of the pyridyl protons are recorded, especially of X′ H$_6$. Moreover, the upfield shift of H$_3$ that is observed in **2** and has to do with pq's conformational switch from *trans* to *cis* after the chelation, is not observed in **1**. The latter worked as a primal proof for the trans/anti conformation of pq in **1**.

The HMBC ^{1}H–^{15}N spectrum of pq in CDCl$_3$ (Supporting material, S1) was considered as a first probe for the partial charges on the nitrogen atoms of the free ligand that could be extrapolated so as to provide us the necessary proves for the coordinated nitrogen atom in **1**. The aforementioned spectrum contains three inde-

Scheme 2.

pendent *J*-networks, where each nitrogen atom couples across two or three bonds with the adjacent protons. The nitrogen atoms are of the pyridine type, that is they provide only one 2p electron to the conjugated π-electron system involved and they have their lone pairs in the plane of the conjugated system, without participating in
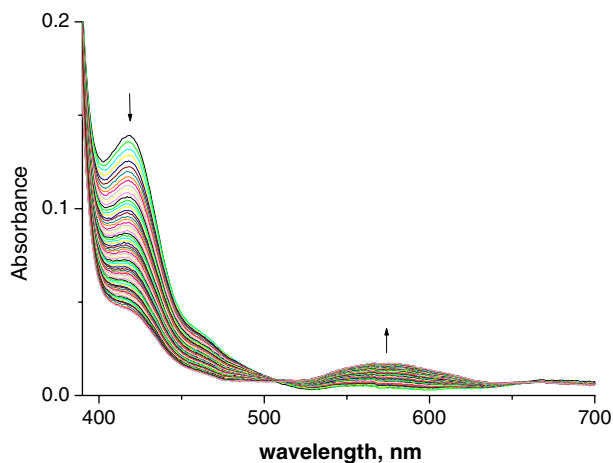

Fig. 1. UV–Vis spectral changes associated with the formation of the $W(CO)_4pq$ chelate complex from $W(CO)_5THF$ in THF at 25 °C in the presence of pq in a ratio 1:10 (thermal reaction).

the delocalized π-electron system. This is illustrated in the positions of the ^{15}N chemical shifts that are characteristic of sp^2 hybridized nitrogens [19]. Unfortunately, N_1 and N_4 cannot be assigned unequivocally, as the long-range connectivity of both N_1 and N_4 with H_3 and correspondingly with H_8 and H_5 are not particularly enlightening, because H_8 and H_5 are NMR equivalent. Nevertheless, it has been reported that the chemical shift of N_4 is relatively insensitive to the different heteroaromatic substituents at the 2-position of the quinoxaline ring [20], while the ^{15}N chemical shift of N_1 is found strongly dependent on these substituents. On this basis, we assign N_4 at 331 ppm, as this chemical shift is closer to corresponding ones of other quinoxaline derivatives. Thus, the most downfield shifted nitrogen atom is N_4 (331 ppm), followed by N_1 (319 ppm) and N_1' (311 ppm) that is also in accordance with the semi-empirically calculated [7n] partial charges on the nitrogen atoms of pq. The planarity of pq [7m] should establish an inter-annular conjugation between its quinoxaline and pyridyl moiety that allows the π-deficient quinoxaline moiety to accept π electron density from the pyridyl ring. This is illustrated by the downfield shift (deshielding) of the pyridine N in pq, in comparison to the ^{15}N chemical shift in the 2-methyl pyridine molecule [19].

The IR spectrum of **1** in DCM shows a CO stretching vibrational pattern (Fig. 2) consistent with the C_{4v} local symmetry of the $W(CO)_5$ skeleton [21] [2073 (w, A_1), 1932 (st, E), and 1904 (m, A_1)]. This pattern changes after the chelation of pq and the formation of **2**. Then four bands at 2011 (A_1), 1906 (B_1), 1882 (A_1) and 1834 (B_2) cm^{-1} appear.

Electronic absorption spectra of **1** in various solvents are indicated in Fig. 3 and the corresponding data are included in Table 3. As a whole, the spectra consist of three main bands; a broad and structured high-energy band extending from 309 to 380 nm, a shoulder at 398 nm and a broad low-energy band. The change of the solvent mainly affects the low-energy band that exhibits negative solvatochromism – that is, it blue-shifts as the polarity of the solvent increases. According to the theory of dielectric polarization, negative solvatochromism is expected for transitions from a ground state with a high dipole moment to an excited state with a smaller one, so that the (di)polar solvents stabilize the GS more than the ES, leading to an increased transition energy [7a].
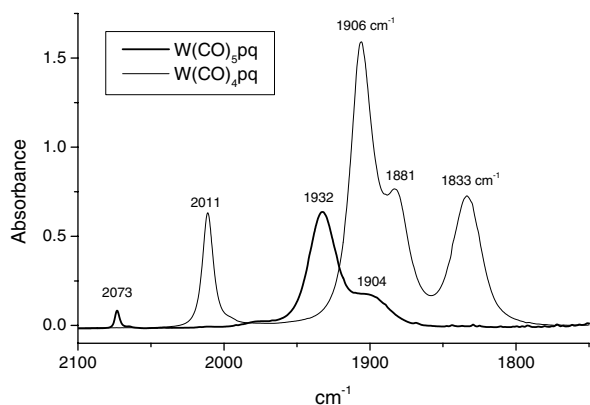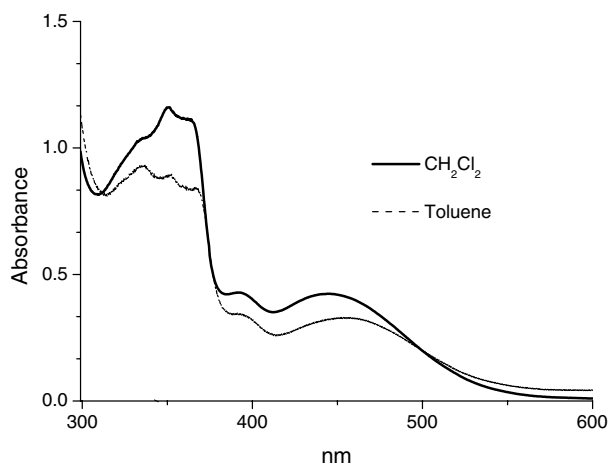
Table 3
Position of the low-energy MLCT band of **1** in various solvents

Solvents	λ_{max} (nm)
CCl_4	483
CH_2Cl_2	446
$CHCl_3$	455
$(CH_3CH_2)_2O$	449
C_6H_{14}	486
Tol	459
THF	424

The shape along with the position and the solvent dependence of the low-energy band denote its $(W)d\pi \rightarrow \pi^*(L)$ charge-transfer (MLCT) character, which agrees with previous interpretations of many mononuclear metal pentacarbonyl complexes [22]. The band seen as a shoulder at ~400 nm that is typically observed for a number of $W(CO)_5L$ complexes [23], would have been traditionally assigned to a ligand-field (LF) $^1A_1(e^4b_2^2) \rightarrow {}^1E(e^3b_2^2a_1^1)$ transition. Though currently, the notation of low-lying LF transitions seems to become abandoned not only for the $W(CO)_5L$ complexes [23] but also for the $W(CO)_4L$ ones [24]. Instead, the interpretation of $W \rightarrow CO$ MLCT states is adopted, contrary to the textbook interpretations. Finally, the resemblance of the high-energy structured band with the band of the free ligand pq implies its $\pi(pq) \rightarrow \pi^*(pq)$ character, though we should not ignore the potential involvement of $W \rightarrow CO$ MLCT transitions.

Room-temperature solutions of **1** do not luminesce, presumably because of rapid ligand dissociation and non-radiative decay to the ground state. Nevertheless, when **1** is excited at 420 nm in a Me-THF glass (77 K), it emits dually (Fig. 4a), with band maxima at approximately 533 and 653 nm and moderate luminescence yields. The two emission bands are poorly separated and both should correspond to short-lived excited states ($\tau < 10$ ns, as this is the limitation of the instrument). For comparison reasons and in order to exclude the possibility that the observed luminescence originates from other species than **1**, we have recorded the emission spectrum of **2** under the same conditions (Me-THF glass, 77 K). After the excitation of **2** at 450 nm, two separate emission bands were received at 573 and 685 nm (Fig. 4b). The high-energy band is particularly broad and rather low in intensity, while the low-energy band is much narrower and intense; both having short lifetimes ($\tau < 10$ ns). As a whole, we conclude that **1** emits at higher energies than **2**, as a result of the difference in coordination around the metal centre. Finally by analogy with $W(CO)_5py$ [23] and $W(CO)_4L$ complexes [24], where dual emission is also observed, we may postulate that the two sets of emission bands of **1** and **2** originate from an interplay of MLCT(L)/MLCT(CO) excited states.

The structure of complex **1**, along with the nitrogen of coordination, was determined by single-crystal X-ray diffraction methods. A suitable crystal of **1** was obtained by recrystallization from DCM/hexane solution. An ORTEP drawing of **1** and its unit cell are shown in Figs. 5 and 6,

Fig. 2. CO stretching vibrational pattern in the IR spectra of complexes **1** and **2** in DCM.

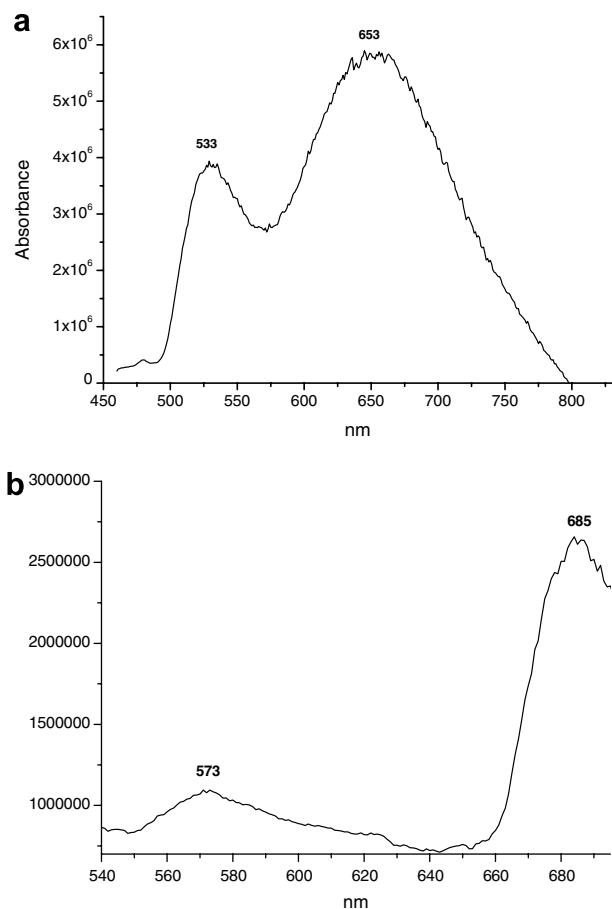Fig. 3. UV–Vis spectra of **1** in toluene and dichloromethane.

Fig. 4. (a) Emission spectrum of **1** in Me-THF glass ($T = 77$ K), excitation wavelength at 420 nm, (b) Emission spectrum of **2** in Me-THF glass ($T = 77$ K), excitation wavelength at 450 nm.
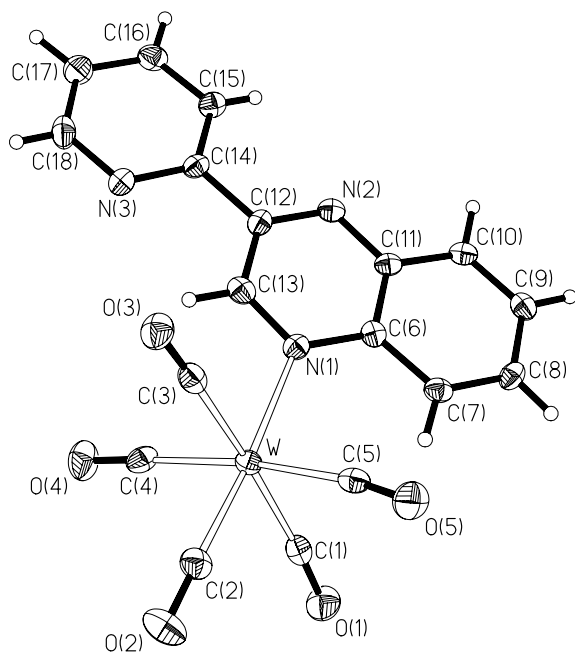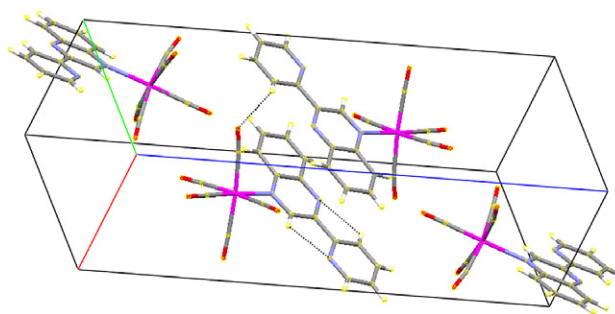

Fig. 6. The unit cell of pentacarbonyl(2,2′-pyridyl-quinoxaline)tungsten, **1**. Some intra- and inter-molecular hydrogen bonds are shown with dash lines.

respectively, and selected bond distances and angles are given in Table 4. The numbering of the atoms in Fig. 5, in Table 4 and in the corresponding discussion of the complex that follows, is different from the one kept for the ligand pq, but still in accordance with IUPAC rules for complexes; attention must be paid that the N_1 atom in the structure of **1** is the same with the N_4 atom in complex **2** [13].

The structure is based on mononuclear units with four molecules of the complex in the unit cell. The molecule has C_1 symmetry. The tungsten is hexa-coordinated through the ring nitrogen atom, an axial carbon monoxide group (CO) and four equatorial carbon monoxide groups. The $W(CO)_5$ fragment is coordinated at N_4 that belongs to the quinoxaline moiety of the diimine ligand. The non-coordinated pyridyl ring is almost coplanar to the complexed quinoxaline moiety [2.1^0(2)], which probably maximizes packing.

In view of the greater negative charge of N_1' and N_1 in comparison with N_4 – supported by the HMBC ^{15}N–^{1}H NMR experiment on pq – the preference of the metal centre to N_4 seems peculiar. On the other hand, reported examples involving poly-aza-ligands have demonstrated that there may be only slight energy differences for low-valent metal fragments such as $W(CO)_5$ between the coordination to a basic, less π-accepting site and the binding to

Fig. 5. An ORTEP drawing of complex **1** with the atomic numbering scheme.

Table 4
Selected molecular parameters (distances in Å, angles in °) of compound (**1**)

Atomic distances (Å)		Atomic angles (°)	
W–N_1 (or W–N_4)	2.311(4)	C_2–W–C_3	88.7(2)
W–C_2	1.959(5)	C_2–W–C_4	86.8(2)
W–C_3	2.043(5)	C_3–W–C_4	90.3(2)
W–C_4	2.047(5)	C_2–W–C_1	85.8(2)
W–C_1	2.048(5)	C_1–W–C_5	88.9(2)
W–C_5	2.049(5)	O_1–C_1–W	172.3(5)
C_1–O_1	1.146(6)	O_2–C_2–W	178.6(5)
C_2–O_2	1.156(6)	O_3–C_3–W	176.9(4)
C_3–O_3	1.140(6)	O_4–C_4–W	176.3(5)
C_4–O_4	1.136(6)	O_5–C_5–W	171.3(4)
C_5–O_5	1.138(6)	C_2–W–N_1	175.62(19)
C_{12}–C_{14}	1.489(7)	C_1–W–N_1	96.98(17)

a less basic but strongly π-accepting coordination center [25]. In our case, the π-electron deficiency of the quinoxaline moiety in respect to the pyridine moiety should enhance the back-bonding, something that may explain the preference for N_4; although N_1' should be more basic than the other atoms, the smaller back-bonding to the pyridyl moiety does not favor the complexation to this.

As it is shown in Fig. 5, the ligand pq demonstrates a *trans*-planar conformation, similar to the one when it is free. The W_1–N_1 (otherwise W_1–N_4) bond distance is 2.311(4) Å, whilst the corresponding axial W_1–C_2 carbon monoxide bond length is 1.959(5) Å. The four equatorial carbon monoxide bond lengths W–C_1, W–C_3, W–C_4 and W–C_5 are 2.048(5) Å, 2.043(5) Å, 2.047(5) Å and 2.049(5) Å, respectively, which are all comparable. The comparison between the structures of **1** and **2** [13] nominates a stronger bonding interaction of W with the pyridyl moiety of pq, as soon as its chelation takes place, as it is seen by the longer W–N_1 bond in **1**, in relation with the W–N_1 in **2**.

It is also interesting to note that the bond angles C_4–W–C_5 (171.3°) and C_1–W–C_3 (174.24°) are smaller than 180°, which results in the bent of the equatorial Cs towards the axial CO. In the same way, the Os of the equatorial COs lean out from the corresponding W–C bonds towards the axial CO. Interestingly the O of the axial CO is almost collinear with W and the corresponding C. The plane of the ligand pq comes between the angles C_4–W–C_3 and C_5–W–C_1, but it does not bisects them. This is indicated by the torsion angle of C_{13}–N_1–W–C_4, which is approximately 40°. This practically means that the plane of pq is approximately 5° closer to the plane of C_3–W–C_1 than to the plane of C_4–W–C_5.

Finally, two internal hydrogen bonds between H_{15}–N_2 [2.548(0.060) Å and 101.59°(4.10)] and H_{13}–N_3 [2.453 (0.54) Å and 103.37°(4.90)] and two intermolecular hydrogen bonds between H's of pq ligand and CO groups [H_7–O_2 2.382(0.054) Å and 132.12°(4.63)and H_{10}–O_3 2.514 (0.060) Å and 164.01°(5.18)] are observed. These H-bonds should also contribute to the particular configuration of **1**, resulting in a novel supramolecular architecture along crystallographic direction.

The major difficulty about the crystallization of **1** has been its inherent instability in solution, which was studied by monitoring its UV–Vis absorption spectral changes. Fig. 7 represents the spectral sequence observed when a 1.1×10^{-4} M solution of **1** in toluene is allowed to stand at 323 K in the dark. Individual spectra were recorded at 30-min intervals. The decay of **1** and the formation of $W(CO)_4(pq)$ **2** (see Eq. (1), Scheme 3) is evidenced by the smooth spectral conversion of the MLCT band of **1** at 456 nm to the characteristic MLCT band of the product complex **2** at 603 nm. The rate of this chelation process (Eq. (1), Scheme 3) has been determined by monitoring the time growth of the MLCT absorption band of **2**. The absorption growth from A_0 to A_∞ vs. time was monoexponentially fitted with correlation coefficients typically greater
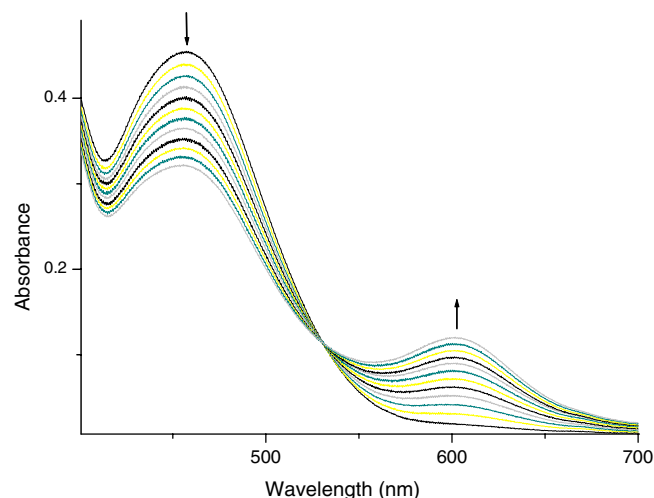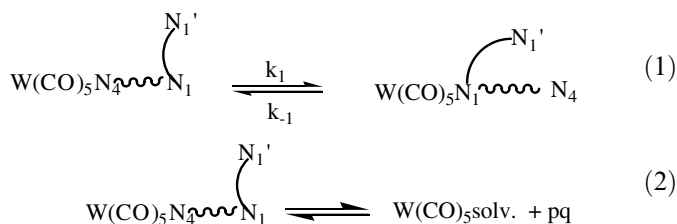

Fig. 7. UV–Vis spectrum of **1** in toluene at 298 K ($\lambda_{max} = 456$ nm). Subsequently occurring spectral changes indicate the formation of the chelate complex **2** ($\lambda_{max} = 603$ nm); note the sharp isosbestic point at 530 nm.

than 0.99 (Supporting material, S2). The estimated reaction rate constant k_{obsd} is 2.3×10^{-5} s^{-1} (at 298 K).

Comparing this rate constant to the data from the literature (Table 5), it is obvious that the nature of the diimine highly influences the stability of the pentacarbonyl complexes. Moreover, the k_{obsd} for the formation of **2** is comparable with previously reported kinetic studies of other $W(CO)_5L$ complexes, where L = ethylenediamine [26], 4,5-diazafluorene [11] and 1,4-diazabutadiene [10e] and suggests the chelation as the rate determined step. But, the smaller k_{obsd} of **1** compared to those of similar complexes with bpy [10e] and the different coordinated nitrogen atoms in both **1** and **2** also indicate that probably a dissociative pre-equilibrium is involved. Actually, the aforementioned differences can be attributed to the fact that a haptotropic shift from N_4 to N_1 needs to take place, which will then lead to the chelation process (Eq. (1)).

$$W(CO)_5N_4\!\!\sim\!\!\sim\!\!N_1 \overset{k_1}{\underset{k_{-1}}{\rightleftharpoons}} W(CO)_5N_1\!\!\sim\!\!\sim\!\!N_4 \qquad (1)$$

$$W(CO)_5N_4\!\!\sim\!\!\sim\!\!N_1 \rightleftharpoons W(CO)_5\text{solv.} + pq \qquad (2)$$

Besides, a bimetallic intermediate as in the case of $Cr(CO)_5(\mu\text{-dmbpy})Cr(CO)_5$ [27] or the solvated $W(CO)_5$ intermediate [28], after the dissociation of pq may precede before the N- switch happens in solution (Eq. (2)). Although present data in toluene (monitored by UV–Vis

$$M(CO)_5(N\text{-}N) \xrightarrow[-CO]{k_{obsd}} (CO)_4M \overset{N}{\underset{N}{<}}$$
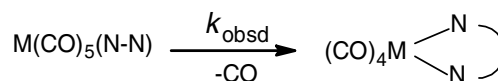
Scheme 3.

Table 5
Observed ring-closure rate constants for various $W(CO)_5L$ complexes in benzene at 293 K

L	k_{obs} (s^{-1})	Isolated	References
Phen	3.6×10^2	n	[10h]
Bpy	3.86×10^{-2}	n	[10e]
4,4′-(CH$_3$)$_2$-bpy	3.51×10^{-2}	n	[10e]
4,4′-(C4H$_9$)$_2$-bpy	1.58×10^{-2}	n	[10e]
4,4′-(C$_6$H$_5$)$_2$-bpy	1.98×10^{-2}	n	[10e]
1,4 – (C$_6$H$_{11}$)$_2$ –dab[a]	1.16×10^{-5}	n	[10e]
1,4 – (C$_3$H$_7$)$_2$ –dab	1.79×10^{-5}	n	[10e]
1,4 – (C$_4$H$_9$)$_2$ – dab	1.05×10^{-4}	n	[10e]
1,4 – (C$_8$H$_9$)$_2$ - dab	4.11×10^{-5}	n	[10e]
daf[b]	8.80×10^{-5}	y	[11]
en[c]	4.2×10^{-5}	y	[26]
Pq	2.3×10^{-5}	y	_[d]

[a] dab = 1,4-diazabutadiene.
[b] daf = 4,5-diazafluorene.
[c] Recorded at 323 K in CHCl$_3$.
[d] Our work.

spectra) do not support any of the aforementioned pre-equilibriums, further kinetic studies, in different solvents and with more advanced techniques are on the way and will be presented in a forthcoming paper.

4. Conclusion

We have managed to isolate, crystallize and study the complex $W(CO)_5(N_4$-pq) (**1**), where pq is mono-coordinated through N_4. This is the first example, where the prosperous ligand **pq** is coordinated in a monodentate fashion. The crystal structure of this complex is unique in the sense that a potentially bidentate pq ligand is mono-coordinated to the $W(CO)_5$ fragment. The dissolution of **1** initiates a decay procedure which affords the tetracarbonyl complex, $W(CO)_4pq$ (**2**) with a k_{obsd} equal to 2.3×10^{-5} s^{-1}.

Acknowledgements

Appendix A. Supplementary data

Figures giving HMBC ^{1}H–^{15}N spectrum of **1** and decay of **1** monitoring by UV–Vis (Figures S1–S2). CCDC 617191 contains the supplementary crystallographic data for $W(CO)_5(N_4$-2,2′-pq). These data can be obtained free of charge via http://www.ccdc.cam.ac.uk/conts/retrieving.html, or from the Cambridge Crystallographic Data Centre, 12 Union Road, Cambridge CB2 1EZ, UK; fax: (+44) 1223-336-033; or e-mail: deposit@ccdc.cam.ac.uk. Supplementary data associated with this article can be found, in the online version, at doi:10.1016/j.jorganchem.2006.09.060.

References

[1] (a) W. Kaim, Angew. Chem., Int. Ed. Engl. 22 (1983) 171;
(b) X.J. Zhao, M. Du, Acta Crystalallogr., Sect. C 59 (2003) 496.
[2] (a) B. Zarranz, A. Jaso, I. Aldana, A. Monge, Bioorg. Med. Chem. 12 (2004) 3711.
[3] (a) M.X. Chen, E. Perzon, N. Robisson, S.K.M. Jönsson, M.R. Andersson, M. Fahlman, M. Berggren, Synth. Metals 146 (2004) 233;
(b) B.L. Lee, T. Yamamoto, Macromolecules 32 (1999) 1375.
[4] (a) D.W. Rangnekar, N.D. Sonawane, Dyes Pigments 45 (2000) 87;
(b) A. Katoh, T. Yoshida, J. Ohkanda, Heterocycles 52 (2000) 911;
(c) R. Touzani, T. Ben-Hadda, S. Elkadiri, A. Ramdani, O. Maury, H. Le Bozec, L. Toupet, P.H. Dixneuf, New J. Chem. 25 (2001) 391.
[5] S.V. Shevchuk, V.M. Lynch, J.L. Sessler, Tetrahedron 60 (2004) 11283, and references therein.
[6] S. Kasselouri, A. Garoufis, A. Katehanakis, G. Kalkanis, S.P. Perlepes, N. Hadjiliadis, Inorg. Chim. Acta 207 (1993) 255.
[7] (a) I. Veroni, A. Rontoyianni, C.A. Mitsopoulou, Dalton Trans. (2003) 255;
(b) C. Shao, W.-H. Sun, Z. Li, Y. Hu, L. Han, Catal. Commun. 3 (2002) 405;
(c) A. Garoufis, S. Kasselouri, C.P. Raptopoulou, Inorg. Chem. Commun. 3 (2000) 251;
(d) A. Garoufis, A. Koutsodimou, C.P. Raptopoulou, A. Simopoulos, N. Katsaros, Polyhedron 18 (1999) 3005;
(e) A. Garoufis, S. Kasselouri, S. Boyatzis, C.P. Raptopoulou, Polyhedron 18 (1999) 1615;
(f) A. Garoufis, A. Koutsodimou, N. Katsaros, C.-A. Mitsopoulou, N. Hadjiliadis, Polyhedron 18 (1998) 361;
(g) S. Kasselouri, A. Garoufis, S.P. Perlepes, F. Lutz, R. Bau, S. Gourbatsis, N. Hadjiliadis, Polyhedron 17 (1998) 1281;
(h) S.P. Perlepes, A. Garoufis, J. Sletten, E.G. Bakalbassis, G. Plakatouras, E. Katsarou, N. Hadjiliadis, Inorg. Chim. Acta 261 (1997) 93;
(i) A. Garoufis, S.P. Perlepes, N.A. Froystein, J. Sletten, N. Hadjiliadis, Polyhedron 15 (1996) 1035;
(j) A. Garoufis, S.P. Perlepes, A. Schreiber, R. Bau, N. Hadjiliadis, Polyhedron 15 (1996) 177;
(k) A. Garoufis, S.P. Perlepes, A. Vreugdenhil, I.S. Butler, N. Hadjiliadis, Inorg. Chim. Acta 240 (1995) 673;
(l) S.P. Perlepes, S. Kasselouri, A. aroufis, F. Lutz, R. Bau, N. Hadjiliadis, Polyhedron 14 (1995) 1461;
(m) S. Kasselouri, A. Garoufis, S. Paschalidou, S.P. Perlepes, I.S. Butler, N. Hadjiliadis, Inorg. Chim. Acta 227 (1994) 129;
(n) E.G. Bakalbassis, J. Mrozinski, S.P. Perlepes, N. Hadjiliadis, F. Lianza, A. Albinati, Polyhedron 13 (1994) 3209;
(o) J.C. Plakatouras, N. Hadjiliadis, S.P. Perlepes, A. Albinati, G. Kalkanis, Polyhedron 12 (1993) 2069;
(p) M.R. Waterland, T.J. Simpson, K.C. Gordon, A.K. Burrell, Dalton Trans. (1998) 185.
[8] (a) C.A. Hunter, Angew. Chem., Int. Ed. Engl. 34 (1995) 1079;
(b) P.J. Stang, D.H. Cao, S. Saito, A.M. Arif, J. Am. Chem. Soc. 117 (1995) 6373, and references therein;
(c) I.Y. Wu, J.T. Lin, J. Luo, S.S. Sun, C.S. Li, K.J. Lin, C. Tsai, C.C. Hsu, J.L. Lin, Organometallics 16 (1997) 2038.
[9] (a) M. Bruschi, P. Fantucci, M. Pizzotti, J. Phys. Chem. A 109 (2005) 9637;
(b) A. Hameed, A. Rybarczyk-Pirek, J. Zakrzewski, J. Organomet. Chem. 656 (2002) 102.
[10] (a) S. Zhang, V. Zang, G.R. Dobson, R. van Eldik, Inorg. Chem. 30 (1991) 355;
(b) Q. Ji, C.R. Lloyd, E.M. Eyring, R. van Eldik, J. Phys. Chem. A 101 (1997) 243;

(c) K.B. Reddy, R. Hoffmann, G. Konya, R. van Eldik, E.M. Eyring, Organometallics 11 (1992) 2319;

(d) R.J. Kazlauskas, M.S. Wrighton, J. Am. Chem. Soc. 104 (1982) 5784;

(e) M.J. Schadt, A.J. Lees, Inorg. Chem. 25 (1986) 672;

(f) M.J. Schadt, N.J. Gresalfi, A.J. Lees, Inorg. Chem. 24 (1985) 2942;

(g) S. Oishi, Organometallics 7 (1988) 1237;

(h) K. Kalyanasundaram, J. Phys. Chem. 92 (1988) 2219.

[11] D.E. Marx, A.J. Lees, Inorg. Chem. 26 (1987) 620.

[12] D.E. Marx, A.J. Lees, Organometallics 5 (1986) 2072.

[13] I. Veroni, C. Makedonas, A. Rontoyianni, C.-A. Mitsopoulou, J. Organomet. Chem. 691 (2006) 267.

[14] D.D. Perrin, W.L.F. Armarego, Purification of Laboratory Chemicals, 3rd ed., Pergamon Press, 1988.

[15] G.M. Sheldrick, SADABS, Bruker AXS Inc., Madison, WI, 1997.

[16] SAINT v5.00, Area Detector Control and Integration Software; Bruker AXS Inc.: Madison, WI, 1998.

[17] G.M. Sheldrick, SHELXTL-97 V5.10, Bruker AXS Inc., Madison, WI, 1997.

[18] W. Strohmeier, F.J. Müller, Chem. Ber 102 (1969) 3608.

[19] M. Witanowski, L. Stefaniak, G.A. WebbNitrogen NMR Spectroscopy, Annual Reports on NMR Spectroscopy, vol. 18, Academic Press, London, 1986, p. 1.

[20] L. Hilfert, G. Sarodnick, G. Kempter, E. Kleinpeter, J. Mol. Struct. 444 (1998) 199.

[21] L.E. Orgell, Inorg. Chem. (1962) 125.

[22] A.J. Lees, A.W. Adamson, J . Am. Chem. Soc. 104 (1982) 3804.

[23] S. Záliš, M. Busby, T. Kotrba, P. Matousek, M. Towrie, A. Vlček Jr., Inorg. Chem. 43 (2004) 1723.

[24] (a) A. Vlček Jr., Coord. Chem. Rev. 230 (2002) 225;

(b) S. Záliš, I.R. Farrel, A. Vlček Jr., J. Am. Chem. Soc. 125 (2003) 4580.

[25] W. Kaim, S. Kohlmann, Inorg. Chem. 29 (1990) 1898.

[26] D.E. Marx, A.J. Lees, Inorg. Chem. 26 (1987) 2254.

[27] (a) B.S. Creaven, F.-W. Grevels, C. Long, Inorg. Chem. 28 (1989) 2231;

(b) F.-W. Grevels, C. Kayran, S. Ozkar, Organometallics 13 (1994) 2937.

[28] (a) R. Perutz, J.J. Turner, J. Am. Chem. Soc. 97 (1975) 4791;

(b) D.R. Tyler, D.P. Petrylak, J. Organomet. Chem. 212 (1981) 389;

(c) M. Brookhart, M.L.H. Green, J. Organomet. Chem. 250 (1983) 395;

(d) J.D. Simon, X. Xie, J. Phys. Chem. 90 (1986) 6751;

(e) J.D. Simon, X. Xie, J. Phys. Chem. 91 (1987) 5538;

(f) Y. Ishikawa, C.E. Brown, P.A. Hackett, D.M. Rayner, Chem. Phys. Lett. 150 (1988) 506;

(g) J.M. Morse Jr., G.H. Parker, T.J. Burkey, Organometallics 8 (1989) 2471;

(h) R. Krishnan, R.H. Schultz, Organometallics 20 (2001) 3314.